

# Optimization of Three Dimensional Culturing of the HepG2 Cell Line in Fibrin Scaffold

Mehrzaad Banihashemi<sup>1</sup>; Milad Mohkam<sup>1,2</sup>; Azam Safari<sup>1</sup>; Navid Nezafat<sup>1</sup>; Manica Negahdaripour<sup>1</sup>; Fatemeh Mohammadi<sup>1,2</sup>; Sedigheh Kianpour<sup>1,2</sup>; Younes Ghasemi<sup>1,2,\*</sup>

<sup>1</sup>Pharmaceutical Sciences Research Center, Shiraz University of Medical Sciences, Shiraz, IR Iran

<sup>2</sup>Department of Pharmaceutical Biotechnology, School of Pharmacy, Shiraz University of Medical Sciences, Shiraz, IR Iran

\*Corresponding Author: Younes Ghasemi, Department of Pharmaceutical Biotechnology, School of Pharmacy, Shiraz University of Medical Sciences, P. O. Box: 71345-1583, Shiraz, IR Iran. Tel: +98-7112426729, E-mail: ghasemiy@sums.ac.ir

Received: August 13, 2014; Revised: November 12, 2014; Accepted: February 22, 2015

**Background:** A potential treatment for healing hepatic tissue is delivering isolated hepatic cells to the site of injury to promote hepatic cells formation. In this technology, providing an appropriate injectable system for delivery of hepatic cells is an important issue. In this regard, fibrin scaffolds were designed with many advantages over other scaffolds like cell delivery vehicles for biodegradation, biocompatibility and hemostasis.

**Objectives:** The aim of this study was to determine suitable cell culture circumstances for HepG2 cell proliferation and differentiation in 3D fibrin scaffolds by evaluating  $\text{Ca}^{2+}$  concentrations, cell numbers, various ratios of plasma/RPMI 1640 and thickness of fibrin scaffold.

**Materials and Methods:** In a one-stage experimental design, Box-Behnken design strategy was performed by Minitab 15 software (version 15, Minitab, State College, PA) with three factors at three levels (low, medium and high) and 27 runs for identification of the effects of ratio of plasma/RPMI 1640,  $\text{Ca}^{2+}$  concentration and thickness on the formation of fibrin gel scaffold and 3D HepG2 culture.

**Results:** The optimal concentrations for fibrin scaffold fabrication were achieved by adding 0.15 mol  $\text{CaCl}_2$  (50  $\mu\text{L}$ ) and  $1 \times 10^5$  cells to 1:4 of plasma/RPMI 1640 ratio (500  $\mu\text{L}$  with 2.3 mm thickness per well).

**Conclusions:** Our approach provided easy handle method using inexpensive materials like human plasma instead of purified fibrinogen to fabricate fibrin scaffold.

**Keywords:** Experimental Design; Fibrin; HepG2 Cells; Plasma

## 1. Background

Tissue engineering is an interdisciplinary field, which combines life and material sciences to restore or maintain tissue functions by means of 3D scaffolds and/or cells (1). The restoring capacity of patient during tissue engineering is enhanced and improved, thereby damaged tissues can be healed and their normal functions can be restored. There are three main therapeutic methods for curing impaired tissues in patients; (I) implantation of freshly cultured or isolated cells, (II) implantation of in vitro cultured tissues from cells and/or scaffolds; and (III) endogenous regeneration (2). In this regard, the methods for tissue engineering are diverse and plentiful, though choosing the proper biomaterial for the scaffold is as important as selection of appropriate cell type (1).

The ideal scaffold should exhibit immunologic integrity, have tissue-like mechanical properties and support cell adhesion, differentiation and migration. The temporary scaffold privileged wipes out via specific degradation, while new tissue is shaped (3). Scaffolds can be fabricated from synthetic materials, natural materials or mixture of them (hybrid scaffolds). Only a few numbers of synthetic

and natural scaffolds show all these features; one of them named fibrin scaffolds. Fibrin is a natural substance with a high potential for application in tissue engineering. Moreover, it can be obtained from patient's own blood to be used as an autologous scaffold, to reduce the potential risk of immunological reaction or infections (4, 5). In vivo, fibrin has a main role in wound healing, inflammation, homeostasis and angiogenesis (6, 7). While in contact with fibrin, cells would progressively substitute the fibrin scaffold by their own extracellular matrix. Taken together, these properties make fibrin an interesting and widely used protein for tissue engineered scaffolds (8).

The features of fibrin scaffolds can be affected by changing the concentration of fibrinogen, thrombin and  $\text{Ca}^{2+}$  during polymerization (9). In addition, concentrations of these fibrin scaffold constituents modulate the way cells differentiate, proliferate and migrate within fibrin (10-12). The optimum conditions of fibrin scaffold were already specified in vitro for nerve cell culture (13, 14), fibroblasts fibrin (10, 15) and mesenchymal stem cells (11). These findings propose that fibrin scaffolds require to be

optimized for each cell type to reduce the number of cell death and promote cell adhesion and migration. However, optimization of fibrin scaffold conditions for hepatic cell was not determined yet.

## 2. Objectives

The aim of this investigation was to optimize fibrin scaffold circumstances using statistical design method (Box-Behnken design) to enhance the proliferation of HepG2 cell line and to assign suitable cell seeding conditions. Moreover, we developed a fibrin scaffold manufactured from plasma as an inexpensive source of fibrinogen and thrombin. This research provided a framework for additional studies about essential factors for shaping hepatic tissue by applying fibrin-matrix scaffolds.

## 3. Materials and Methods

### 3.1. Culture of HepG2 Cells

The human HepG2 cell line (hepatic carcinoma cells) was prepared from the National Cell bank of Iran (NCBI, Pasteur Institute of Iran). HepG2 cells were cultured in 5% CO<sub>2</sub> at 37°C in growth medium [RPMI 1640 (Gibco, Austria) supplemented with 10% (v/v) fetal calf serum (FBS, Gibco/BRL), 10 µg/mL streptomycin and 100 mg/mL penicillin (Sigma, CA, USA)]. Cells were subcultured every 5 - 7 days. Suspensions of HepG2 cells were obtained from mostly confluent cultures (about 80 - 90%) using Trypsin/EDTA solution and cell concentration determined using a hemocytometer. HepG2 cells were inoculated at equal densities directly into wells of a standard 24-well plate (Guangzhou, China). Growth medium was changed every 72 hours as required.

### 3.2. Preparation of Fibrin Scaffolds

Fresh frozen human plasma with normal coagulation parameters and 300 mg/dL fibrinogen concentration and citrate phosphate dextrose adenine (CPDA-1) (as an anticoagulant) was obtained from the Iranian Blood Transfusion Organization. A different volume of plasma/RPMI (1:4, 4:1, and 1:1) was added into each well of the 24-well plate; the ratio of plasma/RPMI is based on the final volume of each well (500, 750 and 1000 µL) shown on Table 1. Various cell numbers ( $2 \times 10^3$ ,  $2 \times 10^4$ , and  $1 \times 10^5$ ) were seeded and followed by adding 50 µL of different CaCl<sub>2</sub> concentrations stocks (0.1, 0.15, and 0.2 mol) per each well and incubated 20 minutes at 37°C in 5% CO<sub>2</sub>. After coagulation and formation of fibrin scaffold, 500 µL of RPMI 1640 media supplemented with 10% FBS was added on top of each scaffold and incubated at 37°C in 5% CO<sub>2</sub>. The growth media was replaced every 24 hours as required.

### 3.3. Optimization Procedure

For achieving the best condition for cell growth and

fibrin scaffold fabrication, Response Surface Methodology (RSM) using Box-Behnken design experiment was applied to identify each key independent variable (16). All the experiments were designed using MINITAB software (version15, PA, USA). Experiments were performed in triplicate and mean values were reported. Finally, the ultimate optimum experimental factors were computed using the Minitab Response Surface Optimizer function, which enables us to distinguish the best combination of each constituent. The designed matrix for four independent variables is exhibited in Table 1. For forecasting the optimal point, a second order polynomial function was fitted to correlate the relationship among independent variables and response for the four factors (concentrations of CaCl<sub>2</sub>, initial cell numbers, and ratios of plasma/RPMI media and various volumes of scaffolds in each of the wells of 24 cell culture plate). This equation is:

$$(1) Y = \beta_0 + \beta_1 X_1 + \beta_2 X_2 + \beta_3 X_3 + \beta_4 X_4 + \beta_{12} X_1 X_2 + \beta_{13} X_1 X_3 + \beta_{14} X_1 X_4 + \beta_{23} X_2 X_3 + \beta_{24} X_2 X_4 + \beta_{34} X_3 X_4 + \beta_{11} X_1^2 + \beta_{22} X_2^2 + \beta_{33} X_3^2 + \beta_{44} X_4^2$$

Where Y is the predicted response,  $\beta_0$  is model constant;  $\beta_1$ ,  $\beta_2$ ,  $\beta_3$  and  $\beta_4$  are linear coefficients;  $X_1$ ,  $X_2$ ,  $X_3$  and  $X_4$  are independent variables;  $\beta_{12}$ ,  $\beta_{13}$ ,  $\beta_{14}$ ,  $\beta_{23}$ ,  $\beta_{24}$  and  $\beta_{34}$  are cross product coefficients and  $\beta_{11}$ ,  $\beta_{22}$ ,  $\beta_{33}$  and  $\beta_{44}$  are quadratic coefficients. The quality of fit of the polynomial model equation was presented by the coefficient of determination R<sup>2</sup>.

### 3.4. Viability Assay

Scaffolds were degraded with fibrinolytic activity of streptokinase (10000IU) in each well for 10 minutes at 37°C until the whole fibrin scaffold was dissolved, and then, cell viability was evaluated by Trypan Blue dye exclusion assay after 10 days of incubation (17).

### 3.5. Function Assay

The functional assays were evaluated by determination of urea secretion after 24 hours in media on the fifth and tenth days using commercial Quantification Kit (Pars Azmoon, Tehran, Iran).

## 4. Results

### 4.1. Morphological Characteristics of HepG2 Cells Grown on Alternative Substrates

The cultivation of HepG2 cell line in routine 2D flask and 3D fibrin scaffold showed significant differences in obtained cells morphology. The grown cells in 2D flask (usually polystyrene surfaces) showed flat extended structures after two days of cultivation. They were also heterogeneous and showed as disarrangement in their appearance. Moreover, after seven days of cultivation, the cells formed aggregates and appeared as unhealthy in which some cells were disintegrating and others were rounding up (data not shown). In contrast,

**Table 1.** Experimental and Predicted Values of Urea Secretion Recorded in the Box-Behnken Design <sup>a</sup>

Trials	Ca <sup>++</sup> , mol	Cell Number	Plasma/RPMI	Volume, $\mu$ L	Urea Secretion, mg/dL			
					Day 5		Day 10	
					Measured	Predicted	Measured	Predicted
1	-1 (0.1)	0 ( $2 \times 10^4$ )	-1 (1:4)	0 (750)	14.30	14.09	15.50	15.49
2	-1 (0.1)	0 ( $2 \times 10^4$ )	1 (4:1)	0 (750)	13.10	13.16	10.80	10.50
3	1 (0.2)	1 ( $1 \times 10^5$ )	0 (4:1)	0 (750)	17.80	17.94	20.25	21.18
4	0 (0.15)	0 ( $2 \times 10^4$ )	0 (4:1)	0 (750)	15.50	15.63	16.30	16.36
5	-1 (0.1)	1 ( $1 \times 10^5$ )	0 (1:1)	0 (750)	15.30	15.05	17.30	16.93
6	-1 (0.1)	0 ( $2 \times 10^4$ )	0 (1:1)	1 (1000)	13.00	13.38	13.50	13.67
7	1 (0.2)	0 ( $2 \times 10^4$ )	0 (1:1)	-1 (500)	15.00	14.78	16.10	16.35
8	0 (0.15)	0 ( $2 \times 10^4$ )	-1 (1:4)	-1 (500)	18.20	17.89	16.50	16.59
9	1 (0.2)	0 ( $2 \times 10^4$ )	1 (4:1)	0 (750)	12.90	13.06	15.00	14.27
10	1 (0.2)	-1 ( $2 \times 10^3$ )	0 (1:1)	0 (750)	13.21	13.32	12.50	13.16
11	0 (0.15)	-1 ( $2 \times 10^3$ )	-1 (1:4)	0 (750)	15.30	15.64	14.75	15.31
12	0 (0.15)	0 ( $2 \times 10^5$ )	1 (4:1)	-1 (500)	13.10	13.31	11.80	13.10
13	0 (0.15)	1 ( $1 \times 10^5$ )	0 (1:1)	1 (1000)	17.40	17.19	16.90	17.30
14	0 (0.15)	0 ( $2 \times 10^4$ )	1 (4:1)	1 (1000)	15.29	15.46	12.50	12.70
15	0 (0.15)	1 ( $1 \times 10^5$ )	0 (1:1)	-1 (500)	18.50	18.36	23.50	21.85
16	0 (0.15)	-1 ( $2 \times 10^3$ )	0 (1:1)	-1 (500)	13.70	13.86	13.50	12.35
17	0 (0.15)	0 ( $2 \times 10^4$ )	0 (1:1)	0 (750)	15.70	15.63	16.60	16.36
18	0 (0.15)	-1 ( $2 \times 10^3$ )	0 (1:1)	1 (1000)	15.15	15.24	14.50	15.40
19	-1 (0.1)	-1 ( $2 \times 10^3$ )	0 (1:1)	0 (750)	13.50	13.22	14.20	13.56
20	-1 (0.1)	0 ( $2 \times 10^4$ )	0 (1:1)	-1 (500)	14.00	14.28	12.50	13.62
21	0 (0.15)	0 ( $2 \times 10^4$ )	0 (1:1)	0 (750)	15.70	15.63	16.20	16.36
22	1 (0.2)	0 ( $2 \times 10^5$ )	0 (1:1)	1 (1000)	16.00	15.88	15.50	14.80
23	0 (0.15)	-1 ( $2 \times 10^3$ )	1 (4:1)	0 (750)	13.50	13.05	11.50	11.14
24	1 (0.2)	0 ( $2 \times 10^5$ )	-1 (1:4)	0 (750)	17.30	17.19	16.00	15.56
25	0 (0.15)	0 ( $2 \times 10^5$ )	-1 (1:4)	1 (1000)	16.30	15.95	16.50	15.49
26	0 (0.15)	1 ( $1 \times 10^5$ )	-1 (1:4)	0 (750)	18.20	18.81	19.20	19.98
27	0 (0.15)	1 ( $1 \times 10^5$ )	1 (4:1)	0 (750)	16.50	16.32	18.00	17.86

<sup>a</sup> The values in parenthesis are the levels of coded variables.

3D cultivation of HepG2 cell line in fibrin scaffold led to more homogeneous cells compared to their 2D counterparts. In this system, HepG2 cell line could intimately interact with the surrounding fibrin scaffold containing plasma and the nutritious environment of human plasma could help these cells to differentiate and proliferate appropriately. Most observed cells in 3D fibrin scaffold had spheroid shape, forming multicellular spheroids (Figure 1). This aggregation is necessary for re-establishment of cell-cell contacts to function as a natural tissue (18). Some researchers reported that existence of extracellular matrices (ECMs) in plasma promoted cell morphologies, phenotypes, differentiated functions and metabolic activities of hepatocytes in a 3D configuration in-vitro (19,20). These data showed that fibrin scaffold containing

human plasma provide an inspiring material for differentiation and cell adhesion studies (21, 22).

#### 4.2. Fibrin Gel Appearance

The initial observation of the formed fibrin scaffold revealed that various combinations of abovementioned factors affected fibrin scaffold appearance. Regarding plasma/RPMI 1640 ratio, gels with a ratio of 1:1 and 4:1 showed a transparent appearance. In contrast, gels prepared with less than 1:1 plasma/RPMI 1640 ratio appeared a little turbid after gelling, were unstable and contracted within ten days of incubation; however, they did not dissolve during this incubation (data not shown). While Ca<sup>2+</sup> concentrations of 0.15 mol and 0.1 mol Ca<sup>2+</sup>

led to transparent gels, fibrin gels containing more than 0.15 mol  $\text{Ca}^{2+}$  were turbid (data not shown). Our results showed consistency with the findings of Eyrich et al. who reported similar results (23). It is suggested that such divalent ions like  $\text{Ca}^{2+}$  affect fibrin gel transparency due to their influences of electrostatic forces and ionic strength, though any increase in  $\text{Ca}^{2+}$  concentration results in fibrin gel turbidity (24, 25). More interestingly, it is reported that variation of parameters for gelation of fibrin scaffold, such as concentration of fibrinogen and thrombin and ionic strength had significantly affected gel appearance, mechanical properties and stability (26).

At very low fibrinogen concentrations (less than 0.5 mg/mL) the fibrin gel appeared turbid, which was related to the large pore size and large fiber diameter (27). In contrast, the opposite impact took place at higher fibrinogen concentrations (1.5 - 23.4 mg/mL) that resulted in finer and stiffer fibrin gels (24). Moreover, changes in thrombin concentrations for 0.001 - 1 U/mL influenced the gel structure (27). However, Eyrich et al. found that variation in thrombin concentration did not affect gel appearance and only affected the speed of polymerization (23). These findings were in agreement with our results showing that normal physiological thrombin concentration (0.9 U/mL) in plasma/RPMI 1640 had no effect on gel appearance.

### 4.3. Determination of Optimal Fibrin Scaffold Components

The response surface methodology using Box-Behnken design was applied to optimize the fibrin scaffold. Four variables including  $\text{Ca}^{2+}$  concentrations, cell numbers, various ratio of plasma/RPMI 1640 and thickness of fibrin scaffold were considered to evaluate the conditions for fibrin scaffold optimization. Urea secretion in culture media was opted as the response for different run series of the runs. Table 1 shows the design matrix for four independent variables for urea secretion in 27 experiments, which were run in three times. Then mean of each response (urea secretion) was computed. The obtained data from the experiments were analyzed by linear multiple regression using Minitab 15 and presented in Tables 2 and 3. The corresponding second-order response model founded after the regression analysis was (Day 5 of incubation):

$$(2) Y_{\text{day5}} = 15.63 + 0.75X_1 + 1.61X_2 - 1.26X_3 + 0.05X_4 - 1.16X_1^2 + 0.41X_2^2 - 0.09X_3^2 + 0.11X_4^2 + 0.69X_1X_2 - 0.80X_1X_3 + 0.50X_1X_4 + 0.02X_2X_3 - 0.6X_2X_4 + 1.02X_3X_4$$

$$(3) Y_{\text{day10}} = 16.36 + 0.96X_1 + 2.85X_2 - 1.57X_3 - 0.37X_4 - 1.13X_1^2 + 0.98X_2^2 - 1.27X_3^2 - 0.61X_4^2 + 1.16X_1X_2 + 0.92X_1X_3 - 0.40X_1X_4 + 0.51X_2X_3 - 1.90X_2X_4 + 0.17X_3X_4$$

Where Y is the predicted response (urea secretion) and  $X_1$ ,  $X_2$ ,  $X_3$  and  $X_4$  are the coded values of  $\text{Ca}^{2+}$  concentration, cell number, plasma/RPMI1640 ratio and thickness, respectively. As illustrated in Tables 4 and 5, relatively high F value and very low P value indicated that the experimental model was in excellent conformity with the experiment for

both responses (day 5 and day 10). ANOVA showed that linear term of the polynomial model was much significant. Data in Tables 4 and 5 show low value of F test and high P value ( $P > 0.05$ ) for lack of fit, which was non-significant indicating that the model is fit. The linear regression coefficients  $R^2 = 0.9795$  and  $0.9351$  and the adjusted determination coefficients  $R^2$  (Adj) were  $0.9556$  and  $0.8594$  for the model (for day 5 and day 10, respectively), which showed accuracy of the model for the Box-Behnken design.  $R^2$  values close to one proposed the robust model resulting in actual values of responses which were closer to the predicted one (16). Among interactive terms for day 5 of incubation, only  $X_2X_3$  did not have a significant influence ( $P > 0.05$ ) on responses (urea secretion), while  $X_1X_3$  ( $\text{Ca}^{2+}$  concentration vs. plasma/RPMI1640 ratio) and  $X_2X_4$  (cell number vs. thickness) coefficient presented a negative effect on HepG2 cell viability (urea secretion for day 5); therefore, they were not suitable for viability of HepG2 cell line. These negative impacts may attribute to the fact that high  $\text{Ca}^{2+}$  provided turbid gels that were more viscous than transparent gels. This higher viscosity may hinder the formation of more densely cross-linked networks leading to failure of withstanding high mechanical loading needed for the cell viability (28). Among the four variables, the plasma/RPMI 1640 ratio and thickness had a negative impact on cell viability. However,  $P > 0.05$  for the thickness means that no significant correlation is present. The detrimental impact of plasma/RPMI 1640 may attribute to the high fibrin concentration, which was proportional to the plasma volume, resulted in a more rigid and dense fibrin gel that halted cell migration and proliferation (11).

Due to the high number of variables, one by one comparison is time consuming and may lead to misinterpretation. Therefore, the final optimum levels of four components were calculated by means of Minitab Response Surface Optimizer function. Optimized values of the factors (for day 5) were found to be:  $\text{Ca}^{2+}$  concentration 0.15 mol, cell number 105, plasma/RPMI 1640 -1:4 and thickness 2.3 mm. A similar pattern was also found for day 10 results. In addition, this model forecasted up to 21.19 mg/dL of urea secretion proportional to the cell viability and activity. By comparing the forecasted and observed values of the Box-Behnken design (Table 1), their good correlation supported precision of the response model and existence of an optimal point (16, 29). However, most researchers investigated optimal conditions for manufacturing fibrin scaffold by means of one-factor-at-a-time methods; there was no report of using statistical design. For the first time, we used the Box-Behnken Design to determine the optimum components for fabricating fibrin scaffold. In this regard, Eyrich et al. reported the optimum fibrin scaffold components as fibrinogen concentration of 25 mg/mL, 3 million cells per construct and  $\text{Ca}^{2+}$  concentration of 20 mM in pH between 6.8 and 9 using one-factor-at-a-time method (23). In a similar study, Willerth et al. found optimal fibrin scaffold constituents of 10 mg/mL for fibrinogen and 2 NIH units/mL of thrombin (9). In another study, Ferreira et al.



evaluated various scaffolds for blood-hematopoietic stem cell expansion and found that fibrin-based scaffold provided the best 3D support, which gave the highest numbers of engraftment and multilineage differentiation in comparison to other 3D biomaterial scaffolds. These features may be due to the efficient cell adhesion to the substrate, which is known to be part of the natural process happening in the liver niche that controls cell proliferation and differentiation. Moreover, this efficient adhesion is sufficient enough for cell migration and homing abilities (30). In comparison to our results, it was concluded that moderate concentration of fibrinogen plus  $\text{Ca}^{2+}$  concentration would result optimum fibrin scaffold, though at this fibrinogen concentration, the proliferation and migration of HepG2 cell line would be occurred optimally.

Additional studies are needed to elucidate other components, which exist in human plasma for better fibrin scaffold manufacturing. In addition, it is necessary to evaluate the immunological reactions to ensure lack or minimum allergenicity. Using human plasma instead of purified fibrinogen provides an easy method for fibrin scaffold fabrication and is considered an economic advantage due to elimination of the costs of purification steps in the preparation of pure fibrinogen with no need for using thrombin. Moreover, in human plasma, some growth factors or other components may exist in human plasma, which are essential for cell proliferation or differentiation.

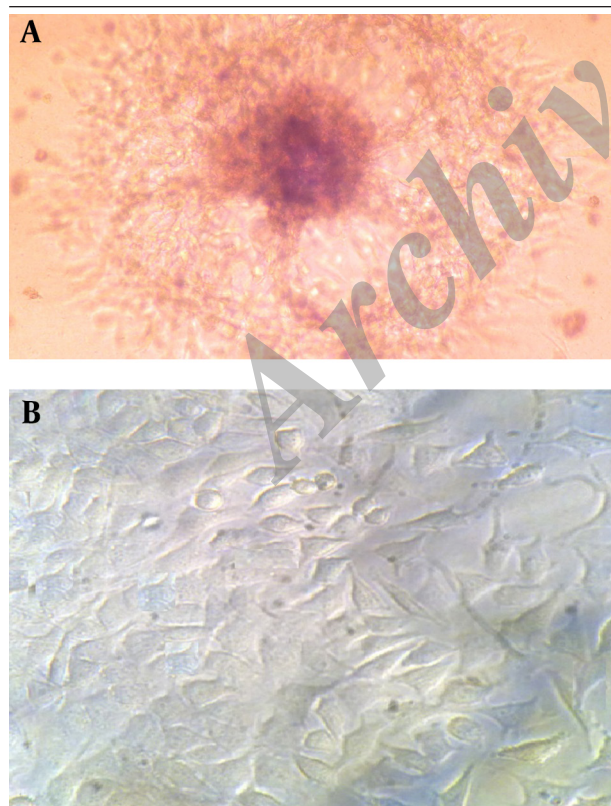


**Figure 1.** Light Microscopy Evaluation of HepG2 Morphology, After 10 Days of Incubation in A) Fibrin Scaffold 10 × and B) in 2D Routine Polystyrene Matrix 40 × (B)

**Table 2.** Statistical Analysis of the Box-Behnken Design for Day Five

Variable	Coefficient	SE-Coefficient	t	P Value
Constant	15.6333	0.2159	72.395	0.000
$X_1$	0.7508	0.1080	6.954	0.000
$X_2$	1.6117	0.1080	14.927	0.000
$X_3$	-1.2675	0.1080	-11.739	0.000
$X_4$	0.0533	0.1080	0.494	0.630
$X_1^2$	-1.1633	0.1620	-7.183	0.000
$X_2^2$	0.4179	0.1620	2.580	0.024
$X_3^2$	-0.0908	0.1620	-0.561	0.585
$X_4^2$	0.1154	0.1620	0.713	0.490
$X_1X_2$	0.6975	0.1870	3.730	0.003
$X_1X_3$	-0.8000	0.1870	-4.278	0.001
$X_1X_4$	0.5000	0.1870	2.674	0.020
$X_2X_3$	0.0250	0.1870	0.134	0.896
$X_2X_4$	-0.6375	0.1870	-3.409	0.005
$X_3X_4$	1.0225	0.1870	5.467	0.000

**Table 3.** Statistical Analysis of the Box-Behnken Design for Day Ten

Variable	Coefficient	SE-Coefficient	T	P Value
Constant	16.3667	0.6107	26.798	0.000
$X_1$	0.9625	0.3054	3.152	0.008
$X_2$	2.8500	0.3054	9.333	0.000
$X_3$	-1.5708	0.3054	-5.144	0.000
$X_4$	-0.3750	0.3054	-1.228	0.243
$X_1^2$	-1.1354	0.4581	-2.479	0.029
$X_2^2$	0.9833	0.4581	2.147	0.053
$X_3^2$	-1.2729	0.4581	-2.779	0.017
$X_4^2$	-0.6167	0.4581	-1.346	0.203
$X_1X_2$	1.1625	0.5289	2.198	0.048
$X_1X_3$	0.9250	0.5289	1.749	0.106
$X_1X_4$	-0.4000	0.5289	-0.756	0.464
$X_2X_3$	0.5125	0.5289	0.969	0.352
$X_2X_4$	-1.9000	0.5289	-3.592	0.004
$X_3X_4$	0.1750	0.5289	0.331	0.746

**Table 4.** ANOVA for the Model That Represents a Secretion Yield From HepG2 in Day Five of Incubation <sup>a</sup>

Source	DF <sup>b</sup>	Sum of Squares	Mean of Squares	F Value	P Value
<b>Regression</b>	14	80.2674	5.7334	40.98	0.000
<b>Linear</b>	4	57.2475	14.3119	102.30	0.000
<b>Square</b>	4	11.7038	2.9259	20.91	0.000
<b>Interaction</b>	6	11.3162	1.8860	13.48	0.000
<b>Residual Error</b>	12	1.6788	0.1399		
<b>Lack-of-Fit</b>	10	1.6521	0.1652	12.39	0.077
<b>Pure Error</b>	2	0.0267	0.0133		
<b>Total</b>	26	81.9462			

<sup>a</sup> Abbreviation: DF, degrees of freedom.<sup>b</sup> Data are presented with  $R^2 = 0.9795$ .**Table 5.** ANOVA for the Model That Represents a Secretion Yield From HepG2 in Day Ten of Incubation <sup>a</sup>

Source	DF <sup>b</sup>	Sum of Squares	Mean of Squares	F Value	P Value
<b>Regression</b>	14	193.462	13.8187	12.35	0.000
<b>Linear</b>	4	139.885	34.9711	31.25	0.000
<b>Square</b>	4	28.496	7.1240	6.37	0.005
<b>Interaction</b>	6	25.081	4.1802	3.74	0.025
<b>Residual Error</b>	12	13.429	1.1190		
<b>Lack-of-Fit</b>	10	13.342	1.3342	30.79	0.075
<b>Pure Error</b>	2	0.087	0.0433		
<b>Total</b>	26	206.890			

<sup>a</sup> Abbreviation: DF, degrees of freedom.<sup>b</sup> Data are presented with  $R^2 = 0.9795$ .

## 5. Discussion

Fibrin is a natural substance with a high potential for application in tissue engineering. Fibrin based scaffold provides the best 3D support and acts as a vector to deliver growth factors and other components that play an essential role in cell proliferation, migration, differentiation and tissue regeneration (30). Wu et al. fabricated self-assembling peptide nanofiber scaffold that can serve as an ideal model for tumorigenesis, growth, local invasion and metastasis, with results comparable to our data. However, ease of manipulation and inexpensive fibrin scaffold could be important advantages in the fabrication of scaffolds (18). In this study, we determined optimal components for the preparation of fibrin scaffold for hepatic tissue engineering. Cultivation of HepG2 cell lines within these 3D scaffolds resulted in the development of an efficient hepatic tissue. These fabricated fibrin scaffolds show appropriate long-term stability providing adequate time for the formation of hepatic tissue as well as human hepatocytes. Moreover, preparation of these fibrin scaffolds from human plasma has advantage over conventional purified fibrinogen due to ease of the process; hence, it is ideal for a wide variety of applications in tissue engineering. However, to use this novel expansion

strategy for human liver transplantation protocols, comprehensive clinical examinations need to be performed to avoid possible side effects. Totally, our approach is a safe and economic method versus previous strategies and has a potential to be used in clinics.

## Funding/Support

This work was supported by the Research Council of Shiraz University of Medical Sciences, Shiraz, Iran.

## References

- Seliktar D. Extracellular stimulation in tissue engineering. *Ann N Y Acad Sci.* 2005;**1047**:386–94.
- Griffith LG, Naughton G. Tissue engineering—current challenges and expanding opportunities. *Science.* 2002;**295**(5557):1009–14.
- Rosso F, Marino G, Giordano A, Barbarisi M, Parmeggiani D, Barbarisi A. Smart materials as scaffolds for tissue engineering. *J Cell Physiol.* 2005;**203**(3):465–70.
- Ahmed TA, Dare EV, Hincke M. Fibrin: a versatile scaffold for tissue engineering applications. *Tissue Eng Part B Rev.* 2008;**14**(2):199–215.
- Jockenhoevel S, Zund G, Hoerstrup SP, Chalabi K, Sachweh JS, Demircan L, et al. Fibrin gel – advantages of a new scaffold in cardiovascular tissue engineering. *Eur J Cardiothorac Surg.* 2001;**19**(4):424–30.
- Weisel JW. Fibrinogen and fibrin. *Adv Protein Chem.* 2005;**70**:247–99.

7. Clark RA. Fibrin is a many splendored thing. *J Invest Dermatol*. 2003;**121**(5):xxi-xxii.
8. Lutolf MP, Hubbell JA. Synthetic biomaterials as instructive extracellular microenvironments for morphogenesis in tissue engineering. *Nat Biotechnol*. 2005;**23**(1):47-55.
9. Willerth SM, Arendas KJ, Gottlieb DI, Sakiyama-Elbert SE. Optimization of fibrin scaffolds for differentiation of murine embryonic stem cells into neural lineage cells. *Biomaterials*. 2006;**27**(36):5990-6003.
10. Cox S, Cole M, Tawil B. Behavior of human dermal fibroblasts in three-dimensional fibrin clots: dependence on fibrinogen and thrombin concentration. *Tissue Eng*. 2004;**10**(5-6):942-54.
11. Bensaid W, Triffitt JT, Blanchat C, Oudina K, Sedel L, Petite H. A biodegradable fibrin scaffold for mesenchymal stem cell transplantation. *Biomaterials*. 2003;**24**(14):2497-502.
12. Yao L, Swartz DD, Gugino SF, Russell JA, Andreadis ST. Fibrin-based tissue-engineered blood vessels: differential effects of biomaterial and culture parameters on mechanical strength and vascular reactivity. *Tissue Eng*. 2005;**11**(7-8):991-1003.
13. Schense JC, Hubbell JA. Three-dimensional migration of neurites is mediated by adhesion site density and affinity. *J Biol Chem*. 2000;**275**(10):6813-8.
14. Herbert CB, Bittner GD, Hubbell JA. Effects of fibrinolysis on neurite growth from dorsal root ganglia cultured in two- and three-dimensional fibrin gels. *J Comp Neurol*. 1996;**365**(3):380-91.
15. Tuan TL, Song A, Chang S, Younai S, Nimni ME. In vitro fibroplasia: matrix contraction, cell growth, and collagen production of fibroblasts cultured in fibrin gels. *Exp Cell Res*. 1996;**223**(1):127-34.
16. Ghasemi Y, Mohkam M, Ghasemian A, Rasoul-Amini S. Experimental design of medium optimization for invertase production by *Pichia sp.* *J Food Sci Technol*. 2014;**51**(2):267-75.
17. Aghdai MH, Jamshidzadeh A, Nematizadeh M, Behzadiannia M, Niknahad H, Amirghofran Z, et al. Evaluating the Effects of Dithiothreitol and Fructose on Cell Viability and Function of Cryopreserved Primary Rat Hepatocytes and HepG2 Cell Line. *Hepat Mon*. 2013;**13**(1).
18. Wu M, Yang Z, Liu Y, Liu B, Zhao X. The 3-D Culture and In Vivo Growth of the Human Hepatocellular Carcinoma Cell Line HepG2 in a Self-Assembling Peptide Nanofiber Scaffold. *J Nanomater*. 2010;**2010**:1-7.
19. Navarro-Alvarez N, Soto-Gutierrez A, Rivas-Carrillo JD, Chen Y, Yamamoto T, Yuasa T, et al. Self-assembling peptide nanofiber as a novel culture system for isolated porcine hepatocytes. *Cell Transplant*. 2006;**15**(10):921-7.
20. Wang S, Nagrath D, Chen PC, Berthiaume F, Yarmush ML. Three-dimensional primary hepatocyte culture in synthetic self-assembling peptide hydrogel. *Tissue Eng Part A*. 2008;**14**(2):227-36.
21. Gelain F, Lomander A, Vescovi AL, Zhang S. Systematic studies of a self-assembling peptide nanofiber scaffold with other scaffolds. *J Nanosci Nanotechnol*. 2007;**7**(2):424-34.
22. Kim MS, Yeon JH, Park JK. A microfluidic platform for 3-dimensional cell culture and cell-based assays. *Biomed Microdevices*. 2007;**9**(1):25-34.
23. Eyrich D, Brandl F, Appel B, Wiese H, Maier G, Wenzel M, et al. Long-term stable fibrin gels for cartilage engineering. *Biomaterials*. 2007;**28**(1):55-65.
24. Ferry JD, Morrison PR. Preparation and Properties of Serum and Plasma Proteins. VIII. The Conversion of Human Fibrinogen to Fibrin under Various Conditions. *J Am Chem Soc*. 1947;**69**(2):388-400.
25. Ferry JD. Structure and Rheology of Fibrin Networks. *Biological and Synthetic Polymer Networks*. Springer; 1988. pp. 41-55.
26. Sidelmann JJ, Gram J, Jespersen J, Kluft C. Fibrin clot formation and lysis: basic mechanisms. *Semin Thromb Hemost*. 2000;**26**(6):605-18.
27. Standeven KF, Ariens RA, Grant PJ. The molecular physiology and pathology of fibrin structure/function. *Blood Rev*. 2005;**19**(5):275-88.
28. Weisel JW. The mechanical properties of fibrin for basic scientists and clinicians. *Biophys Chem*. 2004;**112**(2-3):267-76.
29. Moradpour Z, Ghasemian A, Safari A, Mohkam M, Ghasemi Y. Isolation, molecular identification and statistical optimization of culture condition for a new extracellular cholesterol oxidase-producing strain using response surface methodology. *Ann Microbiol*. 2013;**63**(3):941-50.
30. Ferreira MS, Jähnen-Dechent W, Labude N, Bovi M, Hieronymus T, Zenke M, et al. Cord blood-hematopoietic stem cell expansion in 3D fibrin scaffolds with stromal support. *Biomaterials*. 2012;**33**(29):6987-97.